The structures of carbon nanotubes in their pristine and oxidized form: A quantum chemical model study

S. Irle and K. Morokuma
Emory University, Atlanta, GA, USA, morokuma@emory.edu

ABSTRACT

The molecular and electronic structures of pristine and oxidized [n]cyclacenes (n=6,12) as building element of (n,0) carbon nanotubes have been theoretically investigated. Geometry optimizations have been performed at the B3LYP/6-31G density functional level of theory. For larger systems with three fused [12]cyclacene macrocycles we used the integrated MO-MO (IMOMO) B3LYP/6-31G:RHF/STO-3G level of theory. Reaction products of 1,2- and 1,4-cycloaddition reactions of oxygen atoms with the carbon skeleton served as simple model systems for oxidized systems. The calculated oxidized structures exhibit characteristic deformations as a consequence of change in carbon hybridization, leading to relaxation of ring strain in areas further away from the area of chemical modification.

Keywords: Structural modifications, pristine and oxidized carbon nanotubes, [n]cyclacenes, IMOMO, density functional theory.

1 INTRODUCTION

Since their discovery in 1993,[1,2], single-wall carbon nanotubes (CNT) have received a large amount of attention as top candidates for molecular quantum wires and circuits due to their semiconducting or metallic nature.[3]. It is hoped that such beyond-silicon nanotube electronics may lead to unimagined progress in computing miniaturization and power. However, it has proven difficult to control important factors that determine the electronic structure of CNT's, such as diameter and helicity.[4,5] In addition, it was shown[6,7] that exposure to air and oxygen reduces the nanotube's electrical resistance and increases their thermoelectrical power, but as of yet no detailed structural information is available as to what changes the nanotubes undergo upon oxidation.

The change in electric conductivity has been attributed to chemical doping, namely charge transfer interaction between oxygen molecules and the nanotubes. However, it remains unclear whether the charge transfer is associated with chemisorbed or physisorbed oxygen.

In order to shed light on this question we have chosen to use the density functional level of theory and to carry out geometry optimizations on truncated model systems as representatives of CNT's. We selected macrocycles of six (6,0) and twelve (12,0) fused, fully conjugated C_6 hexagons, using hydrogen as terminating atoms in the axial ("tube") direction. Such monocyclic systems have been postulated as early as 1985[8] and termed [n]cyclacenes (n being the number of hexagons), but so far only precursor molecules without π-conjugation across the entire macrocycle have been synthesized. These structures are commonly regarded as basic cylindical carbon units of one type of CNT's.

Due to the unknown chemical nature of the oxidation sites, we settled for modeling the oxidization of these simple systems by 1,2- and 1,4-cycloaddition products with oxygen atoms, as shown in Scheme 1. We chose these models because they are the smallest possible chemical modification of a nanotube under oxidation with oxygen, and it is also present in lactone groups that are believed to exist in oxidized CNT's.

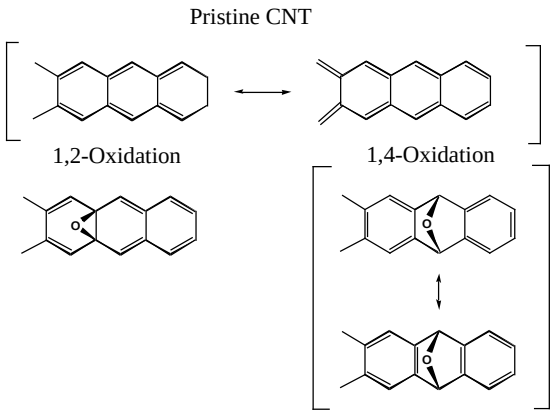

Scheme 1

2 COMPUTATIONAL DETAILS

The geometry optimizations were carried out at the B3LYP level of hybrid density functional theory, using the standard 6-31G basis set with standard *d* polarization functions on oxygen atoms. Benchmark geometry optimizations were also performed for the smaller (6,0) macrocycles using the full 6-31G(d) basis set where polarization functions are included for both carbon and oxygen atoms. As can be seen from Figure 1, the effect of d functions on carbon is mainly a general tendency to shorter C-C bond lengths by up to 0.005 Å, and the energetic differences are minute with 1.5 kcal/mol. Therefore, we felt comfortable in using the simpler 6-31G basis for carbons and to only include polarization functions for oxygen. We denote this basis set 6-31G(Od). Symmetry restrictions were applied, but no imaginary frequencies were found throughout our calculations. The electronic ground state of

most systems studied in this investigation is S_0 closed-shell singlet with the exception of the doubly 1,2-oxidized [12]cyclacene species, which is triplet in its ground state. The singlet-triplet splittings for pristine and 1,2-oxidized forms are small, ranging between -2.5 kcal/mol to 10 kcal/mol.

3 RESULTS

We will discuss the B3LYP/6-31G(Od) energetics and optimized structures for neutral and doubly 1,2- and 1,4-oxidized [6]- and [12]cyclacenes as well as the larger model system for a (12,0) CNT with three hexagon macrocycles in axial direction of the tube. To discuss deviation from the perfectly symmetric structures of pristine systems upon oxidation, it is convenient to define the angles in the projection of the carbon skeleton to the palne perpendicular to the principal axis or in the top view of the structures, as illustrated for pristine **1_6** in Figure 1. The hinge angle η is the projected angle between two hexagones and the bend angle β is the projected angle between the two halves of a single hexagon. For pristine structures with n hexagons arranged in D_{nh} symmetry, the sum η + β has to be 360-(360/n) degrees. Since the largest changes in the carbon skeleton upon oxidation are fairly localized at the positions where carbon atoms directly bound to oxygens, we will call the associated hinge (for the 1,2-oxidized) and bend angle (for the 1,2-oxidized) the "kink" angle, η_k and β_k, respectively. The oxidized species exhibit a characteristic oval shape with two perpendicular diameters of different lengths across the center of the macrocycles. They have to be defined individually for 1,2- and 1,4-oxidized forms. For 1,2-oxidized species, the larger diameter D_l disects to the distance between the two kink hinges with oxygen atoms chemically bound to them on opposite sides of the macrocycle, whereas the shorter diameter D_s is perpendicular to it and is the distance between the center of two hexagons on opposite sides. The situation is reversed in the case of 1,4-oxidized species, where oxygen atoms are located on the center of hexagons on opposite sites with thedistance between them being identical to D_l, whereas D_s is going through the center of the macrocycle perpendicular to D_l. The magnitude of "oval deformation" can then be easily expressed as the ratio between both diameters and is defined here as $R = D_l / D_s$.

The optimized geometries of the six-membered macrocycles are shown in Figure 1. The pristine ring labeled **1_6** possesses D_{6h} symmetry. Its horizontal C-C bonds on top and bottom of the ring are slightly (~0.03 Å) shorter than the vertical bonds, which is consistent with the simple valence formula shown in Scheme 1 and the fact that, unlike in graphite, CNT's show two different bond lengths due to the inequivalence of axial and radial directions. Owing to the relative small size of this macrocycle, the ring strain forces the C_6 hexagons to adapt the bend angle with β=148.5° and a slightly larger hinge angle with η=151.5°, which are 31.5° and 28.5° smaller

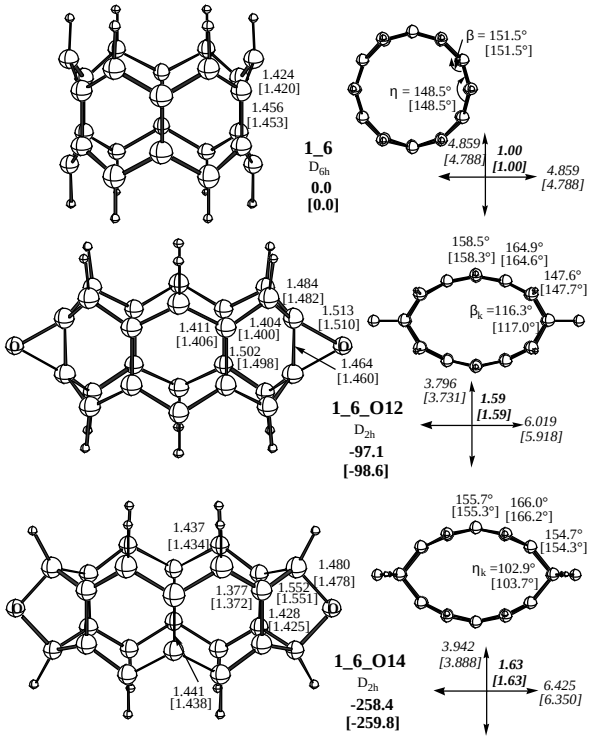

Figure 1

than a planar conformation with β=η=180.0°. As can be seen in Figure 1, each hexagon in **1_6** adapts a boat conformation with top and bottom carbon atoms of the boat pointing away from the center of the macrocycle. When oxygen atoms are added to **1_6** to yield both 1,2- and 1,4-cycloaddition products (**1_6_O12** and **1_6_O14**, respectively), the change in hybridization for the C-O bonded carbon atoms from sp^2 to sp^3 allows substantial relaxation of the ring strain by introducing a kink into the ring system. **1_6_O14** shows the largest deviation from **1_6** with η_k=102.9°, which is decreased by about 46° from η of the pristine system. The kink bend angle of **1_6_O12** is larger with β_k=116.3°, but still reflects a large change in the chemical environment of the oxidized carbon atoms. Due to these kinks, the unaffected C_6 hexagons are allowed to increase both their hinge and bend angles of up to η=164.9° and β=158.5° in **1_6_O12** and up to η=166.0° and β=155.7° in **1_6_O14**. As can be seen in the the top views in Figure 1, the overall effect of kink angles and relaxed hinges and bends is that the formerly cyclic rings are deformed to an oval shape when two oxygen atoms are added on opposite sides and form bonds with sp^3-hybridized carbon atoms. The degree of oval deformation can be readily expressed by the ratio *R* defined above, which is 1.00 for **1_6**, 1.59 for **1_6_O12**, and 1.63 for **1_6_O14**, indicating that the 1,4-adduct is slightly more oval and therefore more relaxed than the 1,2-addition product. The stronger structural relaxation in **1_6_O14** is also reflected in its absolute values of the diameters, both of

which are larger by 0.406 Å and 0.146 Å, respectively than in **1_6_O12**. Upon looking at the bend and hinge angles in **1_6_O12**, one sees that the hinge angle (147.6°) next to the kink is not much different from that in **1_6**, and the relaxation takes place at the next bend angle and further. The situation is also similar in **1_6_O14**; the bend angle (154.7°) next to the kink is not much different from that in **1_6**, and the relaxation takes place at the next hinge angle.

Energetically, the 1,4-adduct is predicted to be more than twice as stable as the 1,2-adduct with a binding energy of 258.4 kcal/mol with respect to pristine **1_6** and two (^{3}P) oxygen atoms as opposed to 97.1 kcal/mol of the 1,2-adduct. The reason for the large energetic difference is twofold. First, the three-membered C-O-C ring in **1_6_O12** is highly strained, whereas the two fused five-membered oxygen-containing rings of **1_6_O14** show no indication of ring strain. In fact, the C-O bond in the latter system is much shorter with 1.480 Å than the corresponding bond in the epoxy system with 1.513 Å, indicating a stronger C-O bond. Secondly, as shown in Scheme 1, the formation of two epoxy groups in the 1,2-cycloaddition reaction with **1_6** destroys aromatic character in four rings, as opposed to only two rings that become affected in the 1,4-cycloaddition reaction. Moreover, π-resonance is formally prohibited in **1_6_O12**. We therefore conclude, that **1_6_O14** would be the preferred product of oxidation reactions with oxygen atoms. However, no matter which of both structures is energetically more stable, it is worth noting that for both systems the ring undergoes a clearly visible structural change as a whole when local sp^3-hybridized centers or defects are formed by addition reactions, reducing the perfect cylindrical symmetry to a lower one.

The 6-31G(d) results for pristine and oxidized [6]cyclacenes are remarkably similar to those with the 6-31G(Od), with carbon-carbon bond lengths slightly shorter when *d*-polarization functions are present. However, the magnitude of the overall change is only about 0.005 Å. Hinge and kink angles are affected only by fractions of a degree, and we therefore felt confident in using the computationally much less expensive 6-31G(dO) basis set.

A six-membered macrocyclic ring with a diameter of only 4.9 Å is certainly too small when comparison is made to real CNT's, where diameters typically range between 11 Å and 15 Å. The (12,0) nanotube model, [12]cyclacene **1_12** as shown in Figure 2, has a diameter of 9.472 Å, and its properties should therefore be closer to real CNT's. As with **1_6**, this macrocycle displays two different bond lengths, 1.411 Å for the horizontal and 1.468 Å for the vertical C-C bonds. The difference between the two is even larger with 0.057 Å than for **1_6**, where it was only 0.032 Å, indicating an even more pronounced resonance stabilization of the longer polyacetylenic substructure. This finding can be related to the fact that firstly the macrocycle is larger, providing more energetical stabilization of the π-conjugated system, and secondly the C_6 hexagons are

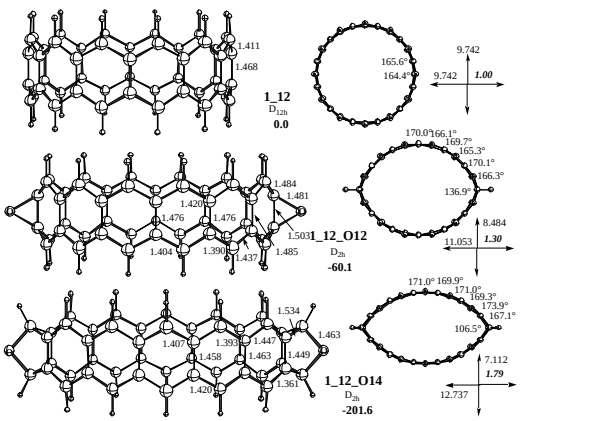

Figure 2

more planar (with β and η being closer to 180° by about 16° and 14°, respectively) than in **1_6** and hence π-overlap becomes more pronounced for this larger system. Upon double 1,2- and 1,4-oxidation leading to products, **1_12_O12** and **1_12_O14,** the cyclic rings in the top view become oval as in the case of the six-membered rings, **1_6_O12** and **1_6_O14**. However, **1_12_O12** is less oval with *R*=1.30 than **1_6_O12** with *R*=1.59, whereas **1_12_O14** has a more pronounced oval shape with *R*=1.79 than **1_6_O14** with *R*=1.63. The reason for the smaller *R* value of **1_12_O12** is the much wider kink angle with β_k = 136.9° as compared to the one of **1_12_O14** with η_k = 106.5° and even the one of **1_6_O12** with β_k = 116.3°. The kink angle in **1_12_O14**, however, is very close to the one found for the six-membered species (η_k = 102.9°). As was the case for the six-membered ring systems, planarization of C_6 units further away from the oxidation site is more pronounced for the 1,4-reaction product. Energetically, the penalty for interruption of the π-conjugation is more severe due to the more planar C_6 hexagons in the pristine system (η = 164.4° vs. 148.5°), and therefore the binding energies are predicted to be lower with 60.1 kcal/mol and 201.6 kcal/mol for **1_12_O12** and **1_12_O14**, respectively. However, the 1,4-adduct remains still twice more stable than the 1,2-adduct, and would be the preferred product.

In order to check how much influence adjecent fused rings in the vertical direction have on the magnitude of structural deformation of the oxidized ring, we replaced the hydrogen atoms of **1_12** with macrocyclic $C_{24}H_{12}$ polyacetylene units and optimized the geometries of pristine **3_12** and 1,2- and 1,4-oxidized **3_12_O12** and **3_12_O14** using the two-layer ONIOM(B3LYP/6-31G(Od):B3LYP/STO-3G) method, as shown in Figure 3. In the ONIOM scheme, **1_12** was chosen as model system for the high level calculation, whereas the entire system was treated at the cheaper B3LYP/STO-3G level. The reason for keeping the B3LYP method in both layers was to eliminate the need for two different scaling factors for frequencies and intensities.

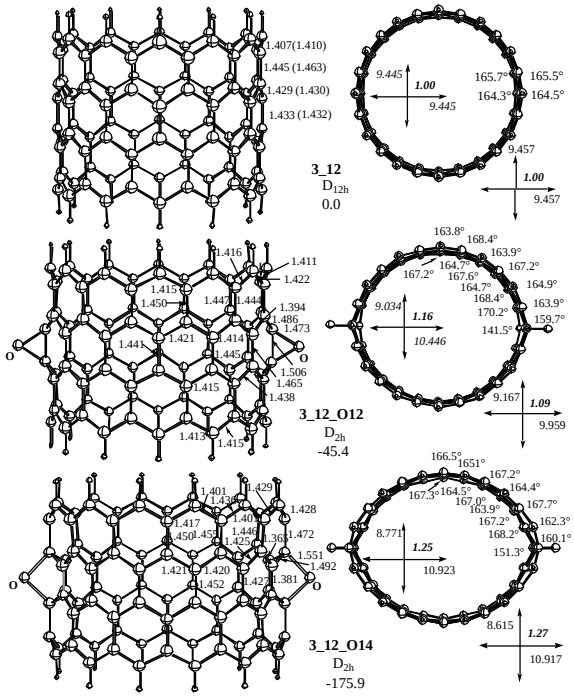

Figure 3

The pristine structure **3_12** displays much smaller C-C bond length differences for vertical and horizontal bonds in its model system **1_12** with 1.433 Å and 1.429 Å than the mono-macrocyclic system itself with 1.456 Å and 1.424 Å, respectively. On the other hand, bond length alternation pattern of the outer rings resembles more closely the one of **1_12**, indicating that edge effects are responsible for the large difference of about 0.05 Å in vertical and horizontal C-C bonds. Therefore one would expect that in the nanotube the difference between the horizontal and vertical bond length would be small. A pure B3LYP/6-31G geometry optimization gives qualitatively the same picture, as shown in parentheses in Figure 3, confirming that the ONIOM method is working well for the present system. Upon examining the oxidation products **3_12_O12** and **3_12_O14**, it is found that the oval shape visible in the oxidized mono-macrocycles is retained also for these extended system, even though the magnitude of deformation is significantly smaller. The ovalicities for inner and outer macrocycles in **3_12_O12** are R_i=1.16 and R_o=1.09, respectively, while **3_12_O14** shows values of R_i=1.25 and R_o=1.27. The inner kink angle is opened up from 106.5° in **1_12_O14** to 151.3° in **3_12_O14**; this is because the outer layer carbon bound to the oxidized sp^3 carbon in **3_12_O14** prevent the latter from twisting outward (as in **1_12_O14**), as seen clearly upon comparison of the top views of the two structures. Interestingly, the hine angle between the two C_6 hexagons immediately above and below the inner kink angle is quite large with β = 160.1°, which indicates that the outer sections of the belt are able to relax strain efficiently, even though the oval shape is preserved. In going away from the oxidation site, the outher C_6 torsional angles are very similar in magnitude and alternation pattern to the ones of the inner ring. This result suggests that, if localized structural deformation has taken place, the neighboring areas are affected by these changes as well due to the tube's desire to achieve maximum π-overlapping. It is therefore relatively easy to achieve large structural deformations in CNT's by introducing localized defects, especially hybridization changes from sp^2 to sp^3 such as occurs during chemical oxidation.

4 SUMMARY

We have performed *ab initio* pure and integrated MO-MO geometry optimization and frequency calculations on [6]- and [12]-cyclacenes as model systems for single walled carbon nanotubes. Oxygen atoms were placed on opposite sides of the macrocycle to model the influence of oxidation on the molecular structures and calculated Raman spectra. It was found that 1,4-oxidization results in much larger binding energies and more stable structures than the 1,2-oxidized analogs. This finding can be rationalized by the larger area of remaining π−conjugation visible in the geometrical parameters for **O14**-type species. The effects of oxygen doping on the molecular structures of these model structures for nanotubes is considerable, actually flatten the non-affected parts of the rings by introducing sp^3-type carbon atoms which make the formerly rigid macrocycle structure more flexible. This effect is even more pronounced for **O14**-type structures than for the **O12**-species and is accompanied by a major decrease in the Raman activities of the carbon skeleton motions. Based on these model calculations we postulate that the sp^3-type defects introduced by chemical oxidation lead to major changes in the nanostructure

REFERENCES

[1] T. Ichihashi, S. Iijima, *Nature* **363,** 603 (1993).
[2] D. S. Bethune, M. S. deVries, G. Goreman, R. Savoy, J. Vazquez, R. Beyers, *Nature* **363,** 605 (1993).
[3] A. B. Dalton, J. N. Coleman, B. McCarthy, P. M. Ajayan, S. Lefrant, P. Bernier, W. Blau, H. J. Byme, *J. Phys. Chem. B* **104,** 10012 (2000).
[4] M. S. Dresselhaus, P. C. Eklund, *Science of Fullerenes and Carbon Nanotubes* (Academic Press, New York, 1996).
[5] R. Saito, M. S. Dresselhaus, *Physical Properties of Carbon Nanotubes* (Imperial College Press, London, 1998).
[6] P. G. Collins, M. Ishigami, A. Zettl, *Science* **287,** 1801 (2000).
[7] F. J. Kong, C. Zhou, M. G. Chapline, S. Peng, K. Cho, H. Dai, *Science* **287,** 622 (2000).
[8] R. W. Alder, *J. Chem. Soc. Perkin Trans. II* **1985,** 1849-1854 (1985).